



This document was produced by scanning the original publication.

Ce document est le produit d'une numérisation par balayage de la publication originale.

GEOLOGICAL SURVEY OF CANADA
PAPER 90-18

EVOLUTION OF SURPRISE RAPIDS LANDSLIDE, YUKON TERRITORY

Brent C. Ward, Lionel E. Jackson, Jr., and K.Wayne Savigny



1992

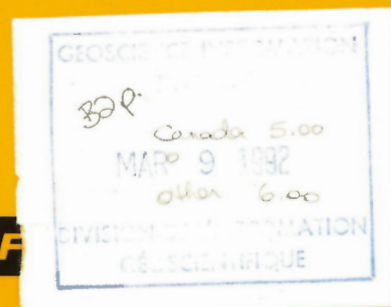


Energy, Mines and
Resources Canada

Énergie, Mines et
Ressources Canada

THE ENERGY OF OUR RESOURCES

THE POWER OF



GEOLOGICAL SURVEY OF CANADA
PAPER 90-18

**EVOLUTION OF SURPRISE RAPIDS LANDSLIDE,
YUKON TERRITORY**

Brent C. Ward, Lionel E. Jackson, Jr. and K. Wayne Savigny

1992

©Minister of Supply and Services Canada 1992

Available in Canada through

authorized bookstore agents and other bookstores

or by mail from

Canada Communication Group - Publishing
Ottawa, Canada K1A 0S9

and from

Geological Survey of Canada offices:

601 Booth Street
Ottawa, Canada K1A 0E8

3303-33rd Street N.W.,
Calgary, Alberta T2L 2A7

100 West Pender Street
Vancouver, B.C. V6B 1R8

A deposit copy of this publication is also available for reference
in public libraries across Canada

Cat. No. M44-90/18E
ISBN 0-660-14380-1

Price subject to change without notice

Cover description

Surprise Rapids landslide, looking east at the margin of a large earth flow (element 6) which moved from right to left in 1977.

Critical Reader

J.A. Heginbottom

Authors' addresses

Brent C. Ward
Department of Geology,
University of Alberta,
Edmonton, Alberta,
T6G 2E3

Lionel E. Jackson, Jr.
Geological Survey of Canada,
Terrain Sciences Division,
100 West Pender St.,
Vancouver, B.C.,
V6B 1R8

K. Wayne Savigny
Department of Geological Sciences,
University of British Columbia,
Vancouver, B.C.,
V6T 1W5

Original manuscript received: 1989-01-13
Final version approved for publication: 1990-07-13

CONTENTS

| | |
|----|--|
| 1 | Abstract/Résumé |
| 1 | Introduction |
| 1 | Setting |
| 4 | Methods |
| 4 | Dendrogeomorphology |
| 4 | Dendrogeomorphic samples, counting, and error |
| 4 | Description of the slide |
| 4 | Landslide materials |
| 9 | Geomorphic elements |
| 10 | Geomorphic element 1 |
| 11 | Geomorphic element 2 |
| 11 | Geomorphic element 3 |
| 11 | Geomorphic element 4 |
| 12 | Geomorphic element 5 |
| 12 | Geomorphic element 6 |
| 13 | Geomorphic element 7 |
| 14 | Timing of events |
| 14 | Element 1 |
| 14 | Elements 2 and 4 |
| 15 | Elements 3 and 5 |
| 20 | Elements 6 and 7 |
| 20 | Chronology and modes of failure of Surprise Rapids landslide |
| 20 | Initial failures |
| 20 | Contemporary failure |
| 20 | Headscarp failure |
| 21 | Failure of element 1 |
| 22 | Remobilization |
| 23 | Discussion |
| 23 | Conclusions |
| 23 | Acknowledgements |
| 23 | References |
| | Appendix |
| 25 | 1. Responses of trees to geomorphic processes |
| | Figures |
| 2 | 1. Location of Surprise Rapids landslide |
| 3 | 2. Map of Surprise Rapids landslide showing geographic elements and sample locations |
| 5 | 3. Airphoto of Surprise Rapids landslide in 1949 |
| 6 | 4. Airphoto of Surprise Rapids landslide in 1950 |
| 7 | 5. Airphoto of Surprise Rapids landslide in 1968 |
| 8 | 6. Low-level oblique photo of Surprise Rapids landslide in 1988 |
| 8 | 7. Distinctive scar on section from tree 86-49 |
| 8 | 8. Complex reaction wood from sections of trees from Surprise Rapids landslide |
| 9 | 9A. Tree X-11 inclined by impact of another tree |
| 9 | 9B. Section from tree X-11 |

| | |
|----|--|
| 10 | 10. Ternary diagram of diamicton and till samples |
| 10 | 11. Liquid limit plotted against plasticity index for diamicton and till samples |
| 11 | 12. Levee system associated with element 6 |
| 11 | 13. Steep face of element 1 |
| 12 | 14. Low, gentle relief of element 2 |
| 12 | 15. Extreme relief of element 6 |
| 13 | 16. Active failure of part of element 3 |
| 13 | 17. Upper part of element 6 showing three stages in its development |
| 14 | 18. Irregular surface of the first stage of element 6 |
| 14 | 19. Major failure of element 1 |
| 15 | 20. View southwest from central portion of element 7 |
| 16 | 21. Composite event and response diagram |
| 17 | 22. Frequency plot for ages of tree samples |
| 19 | 23. Headward sapping by springs along element 1 |
| 21 | 24. Overturned bed of White River Ash in the face of element 1 |
| 21 | 25. Standing water of element 7 |
| 22 | 26. Mean monthly temperatures for Dawson and Mayo |

Tables

| | |
|----|--|
| 2 | 1. Climatic summary |
| 15 | 2. Radiocarbon dates from beneath element 1 |
| 18 | 3. Flow chronology for elements 2 and 4 |
| 19 | 4. Failure event chronology for elements 3 and 5 |

EVOLUTION OF SURPRISE RAPIDS LANDSLIDE, YUKON TERRITORY

Abstract

The Surprise Rapids landslide is a complex of earthflows and debris flows covering an area of about 1.7 km². This failure is the most extensive of its kind in central Yukon. The cause of the initial failure at the site is unknown. Subsequent growth involved bimodal flows and reactivation of landslide colluvium. Debris flows and earthflows were extremely mobile traversing slopes as low as 3°. Landsliding likely began in the 1870s, after a forest fire had swept the site. The landslide involves seven geomorphic elements based upon chronological order of major failure events. Earth and debris flow activity was greatest during the second, fourth, and seventh decades of this century. Landsliding has been coincident with post Little Ice Age climatic amelioration. Warmer summers, especially during the 1940s may have had a role in accelerating the flow of the earth and debris.

Résumé

Le glissement de terrain des rapides Surprise est un complexe de coulées en masse et de coulées de débris, qui couvre une superficie d'environ 1,7 km². C'est la plus vaste rupture de ce genre dans le centre du Yukon. On ignore la cause de la rupture initiale. Par la suite, il s'est produit des coulées bimodales et une réactivation des colluvions de glissement. Les coulées en masse et de débris, qui étaient extrêmement mobiles, ont réussi à traverser des pentes aussi faibles que 3°. Le terrain a vraisemblablement commencé à glisser dans les années 1870, après qu'un feu de forêt eût dévasté le site. Il a touché sept éléments géomorphologiques, à en juger par l'ordre chronologique des ruptures majeures. Les coulées en masse et de débris ont été les plus actives au cours des deuxième, quatrième et septième décennies du XX^e siècle. Les glissements de terrain ont coïncidé avec le réchauffement du climat après le Petit âge glaciaire. Les étés plus chauds, notamment durant les années 1940, pourraient avoir contribué à l'accélération des coulées en masse et de débris.

INTRODUCTION

The *Surprise Rapids landslide* (informal name) is located in the Tay River map area (NTS 105 K) of east-central Yukon (Fig. 1). The location is immediately south of South Macmillan River about 90 km north of the town of Ross River (62°45'40"N, 132°12'00"W).

The landslide is made up of a complex of active and inactive earthflows and debris flows composed of colluvium derived from glacial drift and pedological soil materials. With dimensions of up to 2 km and maximum relief of 240 m, it is the largest complex mass movement in the Macmillan and Pelly river basins. This landslide was investigated to determine its history and the circumstances under which failure has occurred.

Setting

The Surprise Rapids landslide is situated between South Macmillan and Riddell rivers along the western margin of Selwyn Mountains (Fig. 1). The landslide ranges in elevation from about 720 m where it enters South Macmillan River to about 920 m at the highest point in its headscarp, over a distance of about 2100 m. The overall slope of the landslide is approximately 5°, although local slopes below the

headscarp reach 22°. Elevations in the vicinity of the landslide range from 700 m along South Macmillan River to 1100 m along hilltops. North of South Macmillan River, the alpine terrain of the Mount Selous massif rises to over 1900 m. Topography in the area of the landslide is characterized by whaleback ridges formed by the passage of ice. Bedrock is covered by a blanket of till except along and near ridge crests and river banks.

The climate of central Yukon is marked by long, cold winters and short, mild summers. The landslide lies within a region transitional between widespread and sporadic discontinuous permafrost (Johnston, 1981; Permafrost Subcommittee, 1988). Although no permanent weather stations exist near the landslide, records for Tungsten and Ross rivers represent (Table 1) reasonably the climate of this region. Precipitation is almost entirely in the form of snow from October through April and predominantly rain from May through September.

The area surrounding the landslide is forested by black spruce (*Picea mariana*), white spruce (*P. glauca*), and dwarf birch (*Betula glandulosa*). Black spruce dominates under poorly drained conditions and commonly indicates the presence of underlying permafrost. Wet areas are dominated by *Sphagnum* spp. and sedge (*Carex* spp.) bogs.

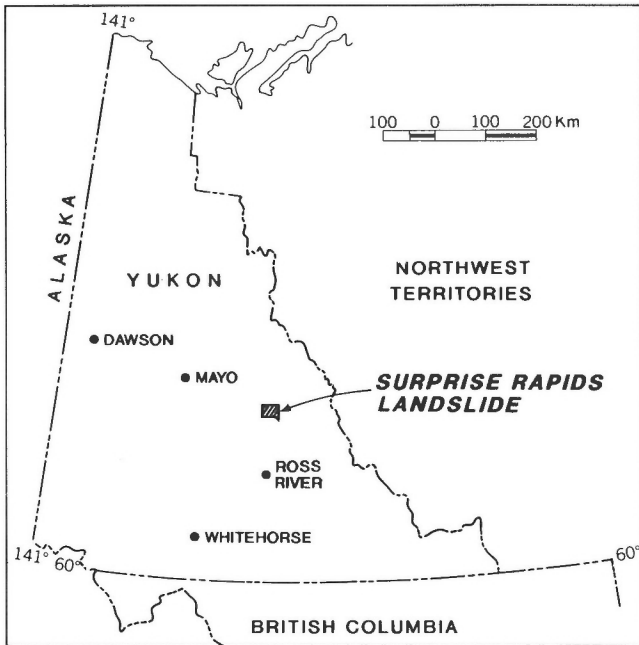


Table 1. Climatic summary

| | Temperature (°C) | | Mean ann precipitation (mm) | |
|---|------------------|------|-----------------------------|-------|
| | Jan | July | | |
| Tungsten, Northwest Territories (61°57' N, 128°15' W, elevation 1143 m)¹ | | | | |
| Daily max | -19.5 | 16.6 | Total | 644.7 |
| Daily min | -29.3 | 5.3 | Snow | 316.7 |
| Annual mean | -5.7 | | Rain | 333.6 |
| Extremes | -50.0 | 27.8 | | |
| Ross River, Northwest Territories (61°59' N, 132°27' W, elevation 698 m)² | | | | |
| Daily max | -23.6 | 21.8 | Total | 263.5 |
| Daily min | -36.1 | 5.3 | Snow | 105.8 |
| Annual mean | -5.7 | | Rain | 152.2 |
| Extremes | -59.4 | 33.3 | | |

¹ Record 10-14 years depending upon parameter measured and the month of measurement.
² Record period is 9-14 years depending upon the parameter measured and month of measurement.

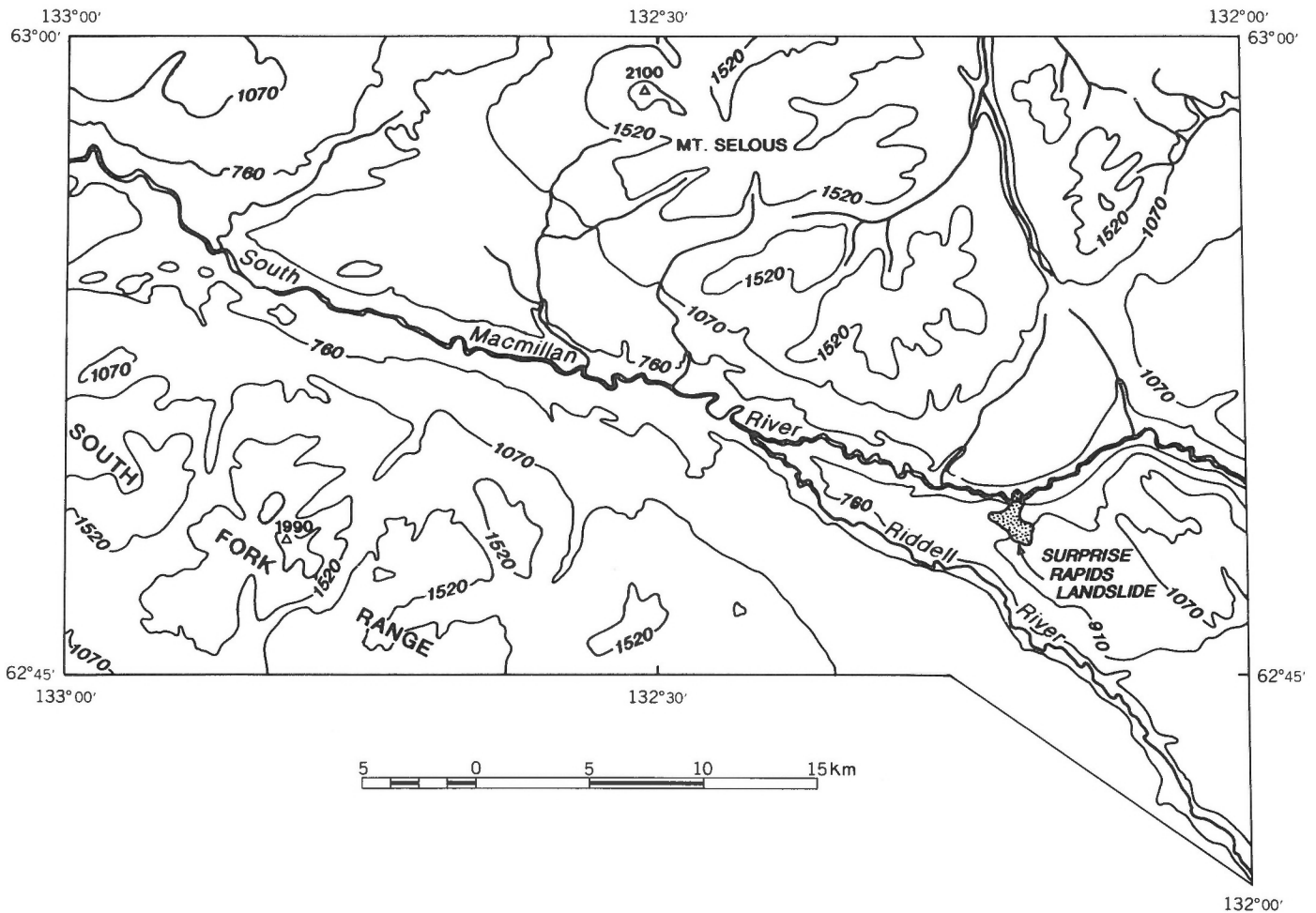
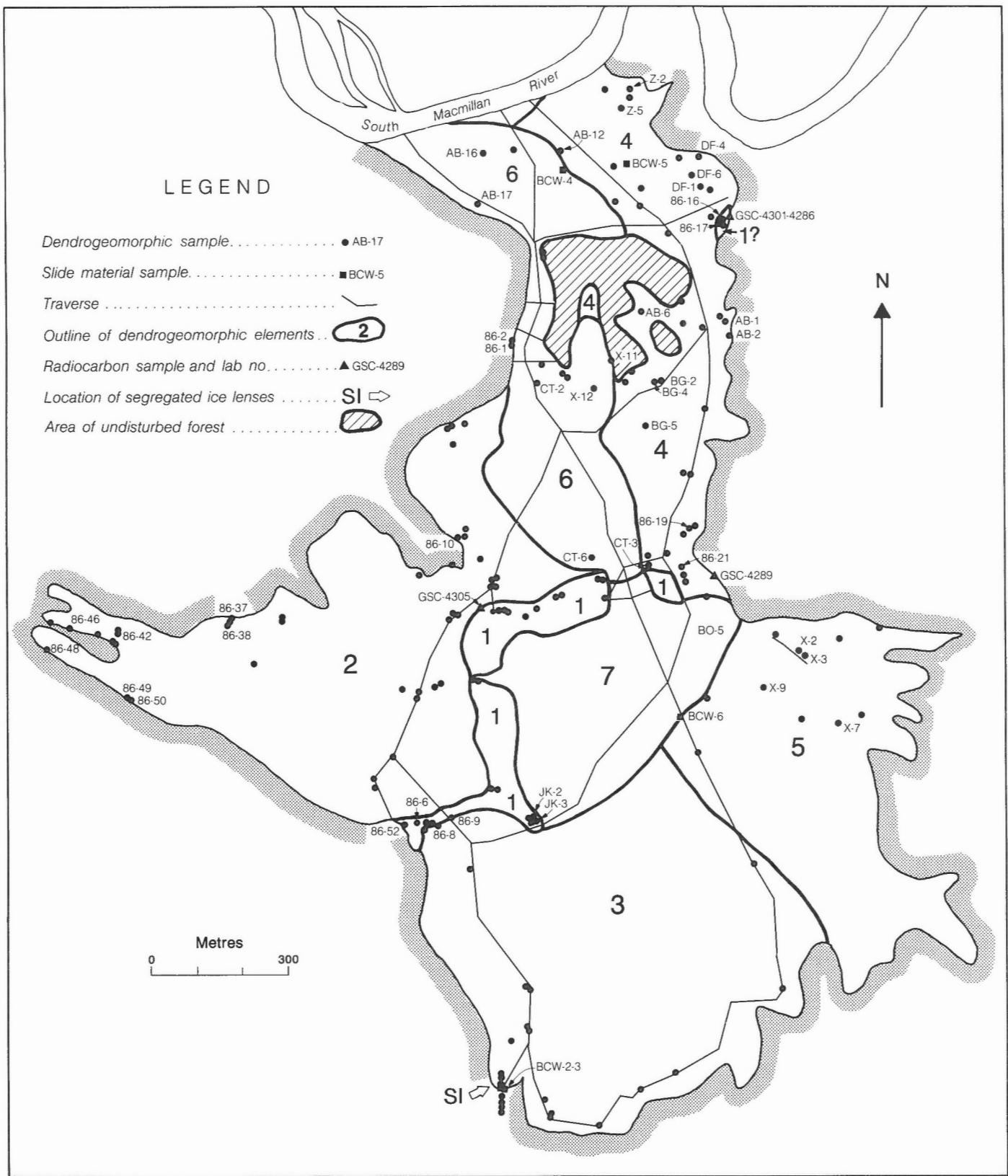


Figure 1. Location of Surprise Rapids landslide.



GSC

Figure 2. Map of Surprise Rapids landslide showing geomorphic elements and the locations of trees used in dating landsliding events.

Pedological soils fall into the Brunisolic, Cryosolic, and Regosolic orders. Brunisols dominate under well drained forest conditions in undisturbed areas or in rafts of soil transported more or less intact within the landslide. Cryosols are present in undisturbed areas where permafrost is within 1 m of the surface. Regosols occur in areas of the landslide now stable. Unstable areas are essentially devoid of any pedological soil development.

The landslide is accessible by helicopter or by boat down South Macmillan River from the North Canal Road 70 km upstream, a dangerous trip through numerous rapids.

Methods

Fieldwork was carried out from July 18 to 27, 1985, June 11 to 14, 1986, and June 24 to 26, 1988. Fieldwork consisted of making a morphological survey of the landslide, sampling of landslide material, investigating of slide stratigraphy, and collecting dendrogeomorphological samples and samples for radiocarbon dating. Transects and sampling points are shown in Figure 2. Dendrogeomorphological sampling points were determined after study of airphotos and the on-site morphological survey. In addition, low level oblique airphotos of the landslide were taken in 1985, 1987, and 1988 (Fig. 6). Radiocarbon-dated stratigraphy as well as dendrogeomorphological samples were used to date events prior to airphoto coverage. Dendrogeomorphological methods are key to unravelling the history and behaviour of Surprise Rapids landslide.

Dendrogeomorphology

Dendrogeomorphology is the study of morphogenic and morphochronological geomorphology using applied plant ecology and dendrochronology (Alestalo, 1971). It is based on the fact that geomorphic processes can cause datable growth responses in trees. These responses have been used to study and date a wide range of geomorphic processes such as glacier fluctuations (Lawrence, 1950); debris flows (Jackson, 1977); slope denudation (La Marche, 1961, 1966); floods (Sigafos, 1964); earthquakes (La Marche and Wallace, 1972); snow avalanches (Potter, 1969); permafrost (Viereck, 1965); tsunamis (Miller, 1960); and eolian activity (Alestalo, 1971). The principles and techniques of dendrogeomorphology are described briefly in Appendix 1. For a more detailed description, refer to Alestalo (1971) and Shroder (1975, 1978, 1980).

In this study, we limited our dendrogeomorphic analysis to examining the growth responses represented by scarring and reaction wood. The events that cause these responses are likely corrasion or impact and inclination, each triggered by one of two geomorphic processes. In the first process, material in the headscarp of the landslide fails, tearing the pedological soil mat and subsequently transporting root-mat fragments downslope as island-like features. This process partially or totally topples trees and trees may be injured, which causes scarring (Fig. 7). Partial toppling also triggers the growth of reaction wood. When downslope movement is slow or episodic, the growth of reaction wood may record

multiple inclination events, including periodic changes in the direction and magnitude of inclination. Multiple events are responsible for complex reaction wood (Fig. 8). When downslope movement is more rapid, the pedological soil mats are deposited on a lower, more level part of the slide during one major event which results in the growth of simple reaction wood. Corrasion of stemwood by slide material, which results in scarring, may occur during any of these phases of movement.

In the second geomorphic process, trees in undisturbed forest are buried by debris flows (Fig. 9). Growth responses triggered by such impacts are more useful in dating landslides than are growth responses triggered by tilting related to transport on the surface of the landslide. Unfortunately, trees surviving debris flows are less common on the Surprise Rapids landslide than are trees recording transportation events.

Dendrogeomorphological samples, counting, and error

A total of 157 *Picea mariana* and *P. glauca* trees were sampled. Most samples (151) were crosscut sections whereas the rest (6) were notch cuts. The surfaces of samples were polished and then examined under a binocular microscope. Event responses were noted and plotted on modified skeletal plots as described by Shroder (1978). The type of conifers we examined usually add one growth ring each year. Aberrant or discontinuous development of annual rings introduces the chief source of error in dendrogeomorphological studies. Partial rings are rings that are discontinuous and are attributable to a stressed growth environment (Stokes and Smiley, 1968). Counting along a radius where a ring is missing results in a date that is too young. A false ring is produced part way through a growing season and consists of a band of smaller cells denser than normal (Stokes and Smiley, 1968). These cells mimic the cells usually formed at the end of the growing season but lack the sharp contact with the subsequent earlywood. If not identified, they result in a date that is too old. To reduce error caused by partial or false rings, each sample was counted along two radii.

The error caused by discontinuous and false rings is assumed to be <5% of the age of the event. Potential errors are minimized where trees from the same geomorphic feature yield the same date.

DESCRIPTION OF THE SLIDE

Landslide materials

With the exception of locally peaty pedological soil and vegetal debris, the Surprise Rapids landslide is composed entirely of colluvium derived from glacial drift. No evidence anywhere in the landslide suggests bedrock involvement. In local stream cuts, the slide is seen to override either undisturbed glacial sediments or the Paleozoic sedimentary bedrock.

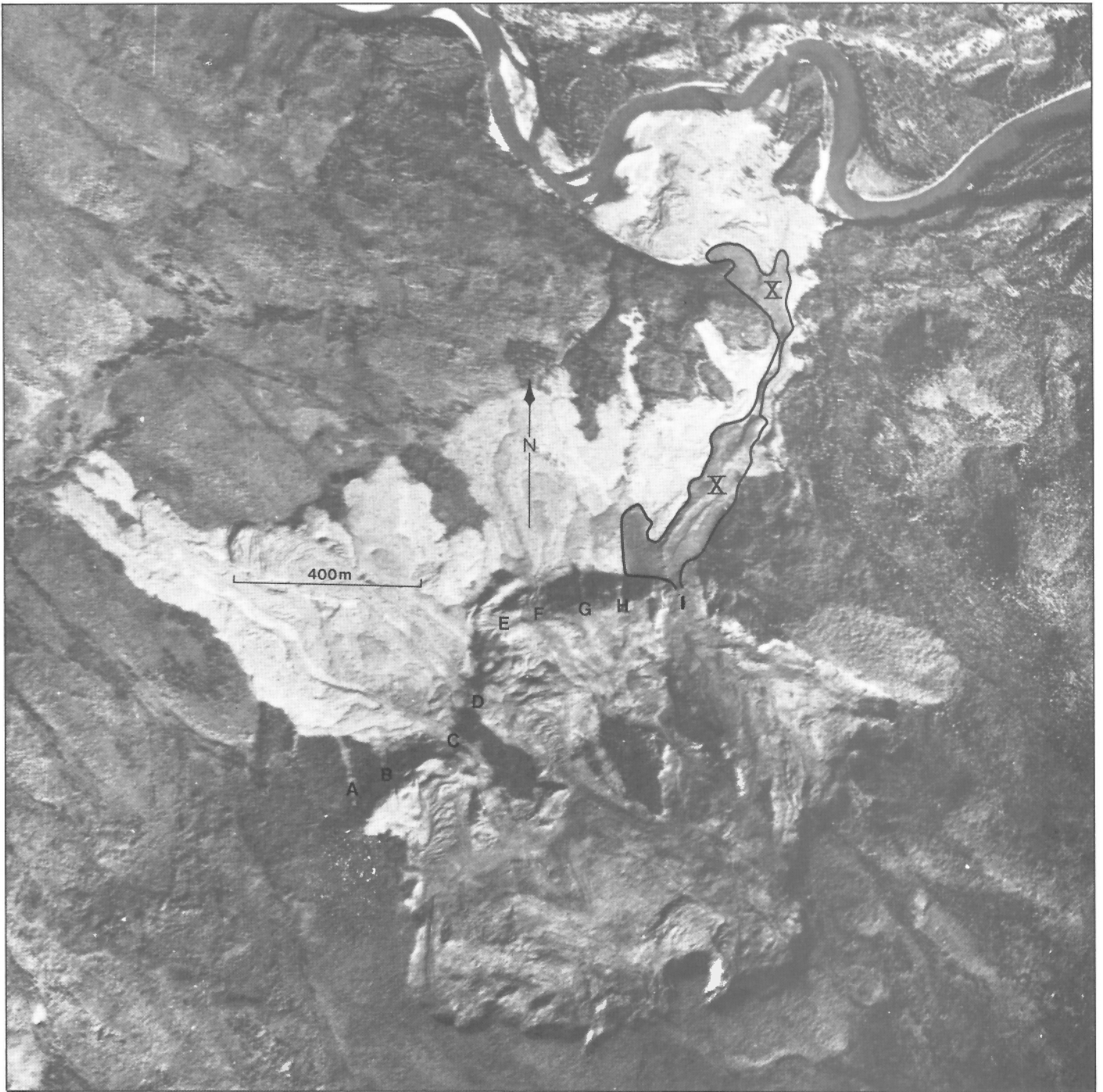


Figure 3. Enlargement of a 1949 airphoto of Surprise Rapids landslide showing geomorphic elements, flow X, and points of overflow over element 1 (A-I), which are discussed in the text. NAPL A12340-417

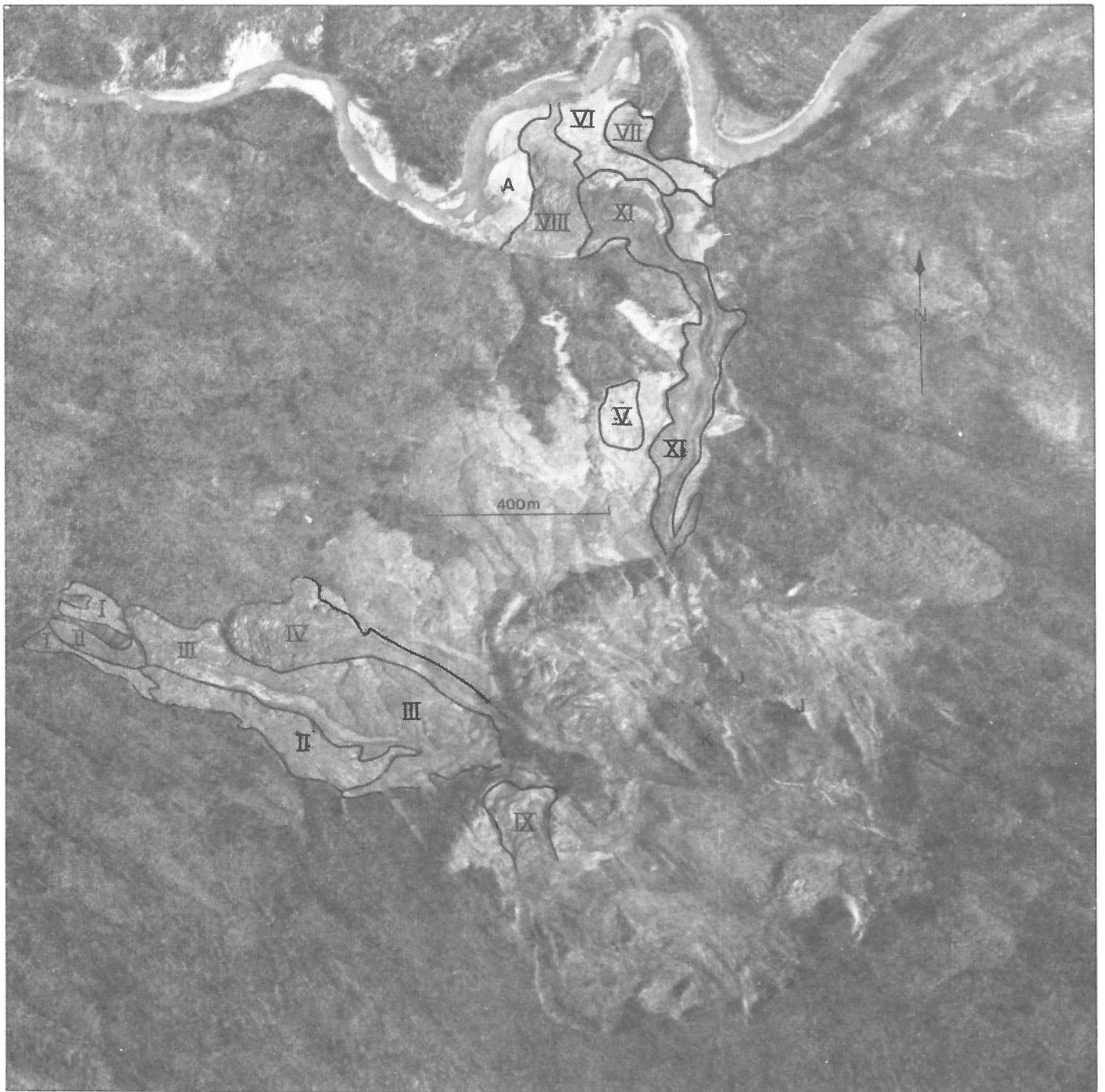


Figure 4. Enlargement of a 1950 airphoto of Surprise Rapids landslide showing geomorphic elements, flows (Roman numerals), and flow source areas (capital letters), which are discussed in the text. NAPL A12850-154



Figure 5. Enlargement of a 1968 airphoto of Surprise Rapids Landslide showing geomorphic elements, flows (Roman numerals), and flow source areas (capital letters), which are discussed in the text. NAPL A20695-100



Figure 6. Low-level oblique photo of Surprise Rapids landslide taken in 1988 showing geomorphic element 6 (dotted line) and geomorphic element 7 (dashed line). Nested levee of element 4 indicated by small arrow. GSC 1991-114

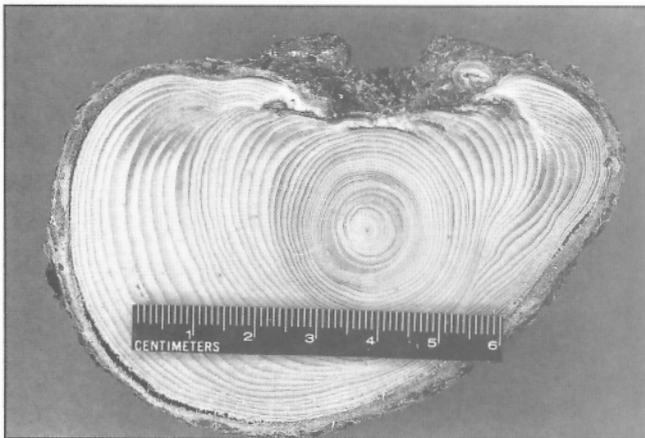


Figure 7. Section from tree 86-49 showing a distinctive scar. GSC 1991-121

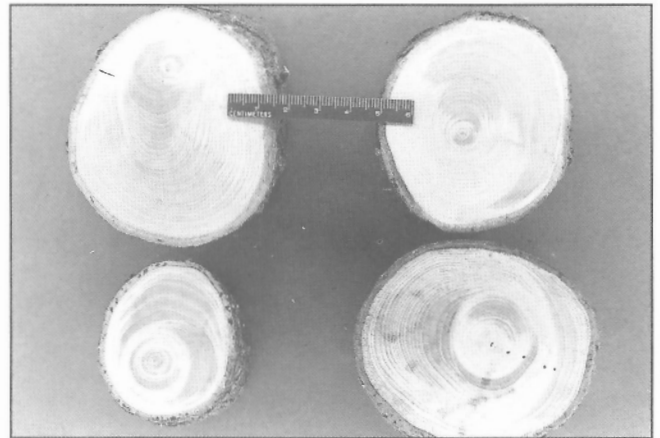


Figure 8. Examples of complex reaction wood from tree sections taken from Surprise Rapids landslide are characteristic of trees sampled from the surface of flows. Complex reaction wood indicates that a tree was inclined or rotated on several occasions. GSC 1991-120

The landslide colluvium is dark grey. Clay content of the <2 mm fraction of four samples taken from widely spaced areas of the landslide range from 49 to 56 weight % (Fig. 10). These values are anomalously clay rich relative to the clay contents of glacial diamictons derived from Selwyn Basin bedrock elsewhere in the region and now exposed in the headscarp of the landslide (Fig. 10). The local bedrock has been inferred to be Earn Group clastics of Devonian-Mississippian age. The Earn Group is not highly argillaceous (S.P. Gordey, personal communication, 1987) so the ultimate source of the high clay content of the colluvium composing the landslide is unknown. A likely explanation for this anomalously high clay content is that a significant part of the landslide was derived from lacustrine or glaciolacustrine sediments rather than glacial diamicton. Further evidence to support this hypothesis is discussed later.

Regardless of its origin, the higher clay content of the landslide colluvium enhances its plasticity relative to glacial diamicton derived from the Paleozoic and Mesozoic

sedimentary rocks of the Selwyn Basin (Gabrielse, 1967) (Fig. 11). Glacial diamictons derived from Selwyn Basin rocks have low plasticity values whereas the landslide colluvium falls within the intermediate range.

The extent of permafrost within landslide colluvium is unknown; however, permafrost was almost certainly extensive in the preexisting slope. Two of the authors (Ward and Jackson) have found permafrost to be almost continuous at elevations and aspects comparable to the Surprise Rapids landslide throughout the Pelly River basin. In 1986, the senior author observed segregated ice lenses within sediments failing in an active area of the headscarp.

Geomorphic elements

The Surprise Rapids landslide is divisible into geomorphic elements of varying ages which have disrupted the vegetative cover of the area. Parts of the slide are actively failing whereas other areas now appear to be stable.

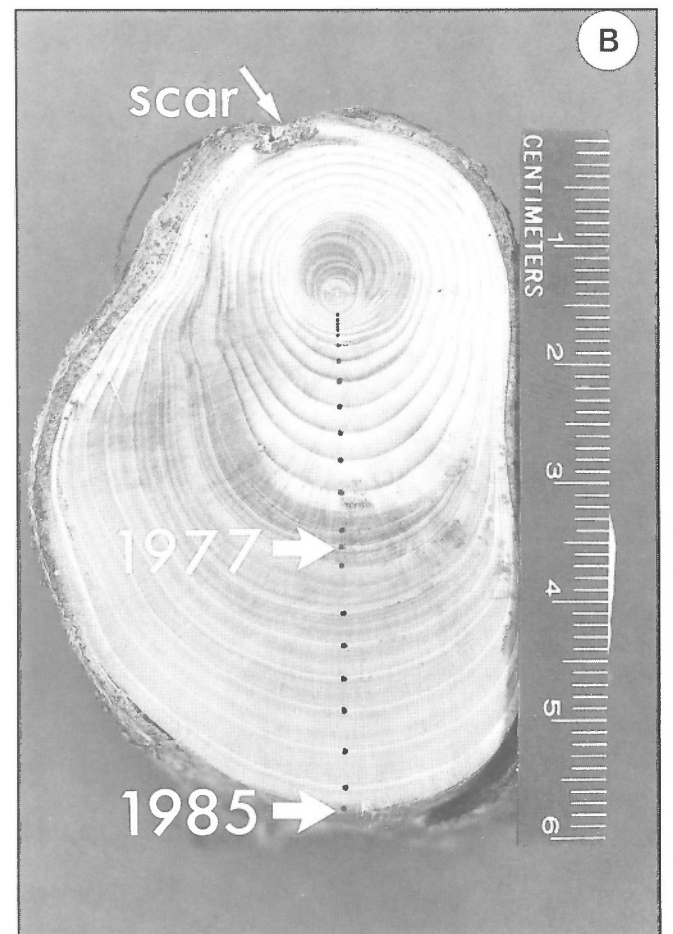


Figure 9. The tree X-11 (A) The tree inclined by the impact of another tree, which had been impacted by landslide activity to the left of the photograph. (B) A section from tree X-11. The impact resulted in minor scarring as well as reaction wood (eccentric dark ring growth) on the opposite side of the tree. Reaction growth started in 1977, which was the time of formation of element 6. Also of interest are the many false rings associated with the reaction wood. Annual rings are denoted by dots. GSC 1991-113

As of June 1986, seven major geomorphic elements were definable (Fig. 2) based upon sharp or truncating contacts between elements and contrasting surface morphology (Figs. 3-6). These were numbered 1 to 7 based upon the chronological order of periods of major failure (1 is the oldest). Entire elements or parts of them are actively failing or have been recently deposited. In depositional zones or zones of transport, active or recently active areas are marked by fresh levees (Fig. 12), ridged and jumbled topography, and debris flow lobes. Other elements appear to have been stable for long periods. Headwall areas are stable and vegetated, whereas former areas of ridged or jumbled topography have been eroded to rounded, rolling, or planar forms. Each of these elements and their relative age relationships (Fig. 2) are described below. Absolute dating of flow events is discussed separately in the section on *Timing of events*.

Geomorphic element 1

Geomorphic element 1 is a rampart-like feature that trends parallel to contour and bisects the slide between about 800 and 820 m elevation. All other elements are either derived from this feature or have partly buried it during their

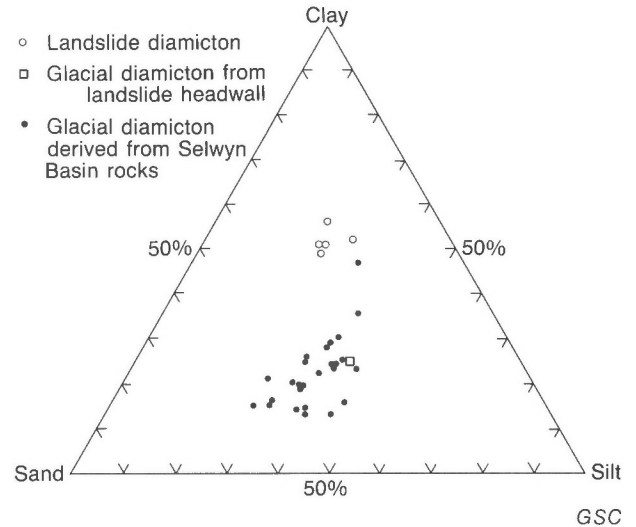


Figure 10. Ternary diagram of landslide diamicton, glacial diamicton sample texture from the headwall of element 5, and the glacial diamicton samples overlying Selwyn Basin (Gabrielse, 1967) sedimentary rocks.

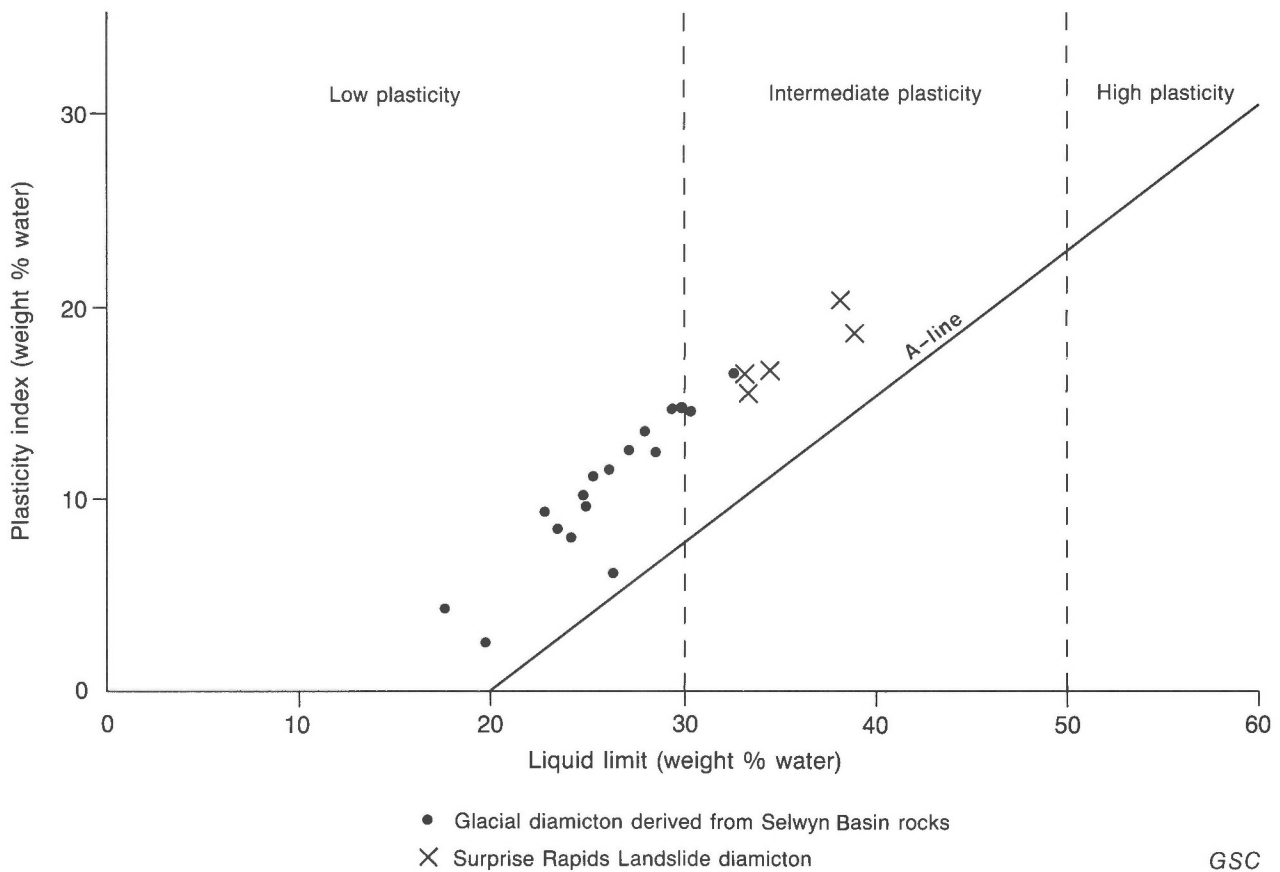


Figure 11. Plot of liquid limit versus plasticity index for landslide diamicton samples and glacial diamicton samples derived from Selwyn Basin sedimentary rocks.

formation. The distal margin of this feature has a steep rounded profile and considerable relief (Fig. 13). Its height above the lower flows ranges from 20 to 25 m with slope angles of between 15° and 55°. Where element 1 has not been buried or itself has failed, it is abundantly forested. Element 1 is composed of a ridge of poorly sorted glaciofluvial gravel and diamicton mantled by landslide colluvium. The ridge originated as a kame, esker, or crevasse filling during deglaciation. Large quantities of landslide diamicton have accumulated behind (upslope) of this ridge. They have flowed through the ridge in two places following local failures.

Geomorphic element 2

Geomorphic element 2 (Fig. 2 to 6) is an apron of many overlapping and interdigitating, generally low relief debris flow lobes and leveed channels. The mean slope of this apron is 3° to 4°. Relief over much of this element ranges from 1.5 m or less over tens of metres between levees to <20 cm over tens of metres on the surfaces of flat-topped flows (Fig. 14). This relief is in contrast to the jagged and jumbled surface of adjacent element 6 (Fig. 15) and the promontory of element 1 (Fig. 13). Element 2 is almost entirely devoid of vegetation with the exception of rafts of vegetation transported on the surfaces of the flows (Fig. 14). Element 2 is buried to the east by element 6. Prior to burial by element 6, (Fig. 3-5) element 2 was continuous with element 4. The debris flows making up element 2 originated as earthflows and debris flows within element 3.

Geomorphic element 3

Geomorphic element 3 is delineated in Figures 2 to 5. It consists of the western half of the headscarp of the landslide whence material forming geomorphic element 2 was derived (levees connecting elements 2 and 3 are indicated by A-F in Fig. 3). The slopes of element 3 range from 4° to 22° but average from 6° to 8°. Its surface morphology ranges from smooth slopes to active and inactive earthflows. Element 3



Figure 12. Looking up the large levee system associated with the second stage of formation of element 6. (The arrow indicates a man 1.8 m tall for scale). GSC 1991-117

is now expanding south into the adjacent upland along its southwestern margin (Fig. 16). The active area of element 3 is characterized by the surface vegetation mat draping over scarp faces (Fig. 16), trees tilting, and blocks of colluvium and pedologic soil material rotating or toppling as they progressively become transformed into earthflows. The total volume of slope material removed from elements 3 and 5, which together make up the headscarp of the landslide, is between 0.8×10^5 and 1.6×10^6 m³ assuming the average thickness of slope removed to be between 1 and 2 m.

Geomorphic element 4

Element 4 extends north to South Macmillan River from the northeastern end of element 1. It descends about 80 m over 1000 m with an average slope of 5°. Element 4 can be subdivided into three subelements: an apron of debris flow lobes extending from directly below element 1 to halfway to South Macmillan River; nested debris flow channels and levees; and a debris flow fan along South Macmillan River, formed of overlapping debris flow lobes. The first subelement was continuous with element 2 before element 6 formed (Fig. 3 to 6). This apron formed when flows from

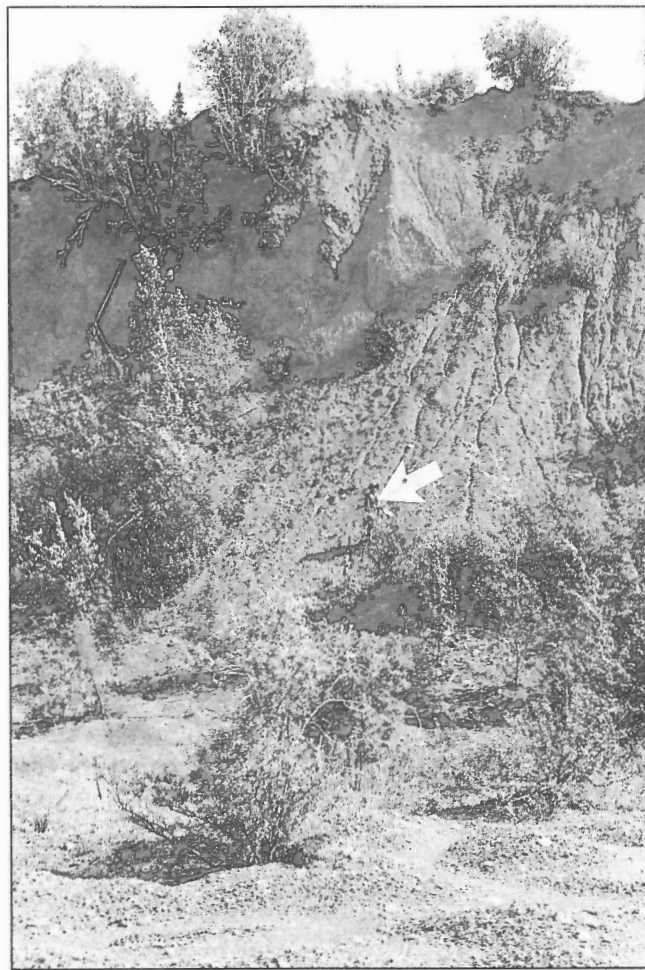


Figure 13. The steep face of element 1 looking east (upslope) from element 2. (The arrow indicates a man for scale.) GSC 1991-115



Figure 14. Panoramic view of element 2 from a promontory atop element 1 looking west to northwest, immediately after a rainstorm. Note the low gentle relief, the relative lack of vegetation, and the well developed drainage pattern. The largest streams follow the edges of lobes. The extensive amount of water on element 2 reflects the high clay content and poor drainage properties of the diamicton composing the landslide. GSC 1991-110

element 5 spilled over element 1 (G and I of Fig. 3). These events were followed by the breaching of a segment of element 1 (H of Fig. 3). The nested levees originated following the failure of element 1 (Fig. 3 and 4). This breach served as a conduit through which all subsequent earthflows and debris flows from the southeast corner of element 5 were funnelled. Material was transported via a large debris flow channel to South Macmillan River, where a large fan formed, affecting the course of the river. This channel, still clearly evident (Fig. 6), is up to 45 m wide and more than 2 m deep near its upper reaches. When the channel was active, debris flows were large enough to overtop the channel and form splay lobes. These were likely formed during the waning stages of debris flow activity on element 4 when small debris flows stalled within the large channel and subsequent flows created new channels around them.

Geomorphic element 5

Element 5, discussed in relation to elements 4, 3, and 1, has much the same relief and overall slope as element 3. All the sediments of element 4 and much of element 6 derive from element 5. The surface of the element ranges from smooth slopes to presently stable and vegetated earthflow lobes. The headwall has not changed significantly from the configuration seen in the 1968 airphoto (Fig. 5 and 6). Unlike element 3, it is not actively expanding into the adjacent upland.

Geomorphic element 6

Geomorphic element 6 (Fig. 2 and 6) is the most recent major failure. Its outline on Figure 2 is approximate, based upon low-level oblique photos and tape and compass traverses. Element 6 formed in three stages with each stage having different surficial morphologies. The first stage involved the catastrophic failure of geomorphic element 1 and earthflows ponded behind it (C of Fig. 3). This failure resulted in an

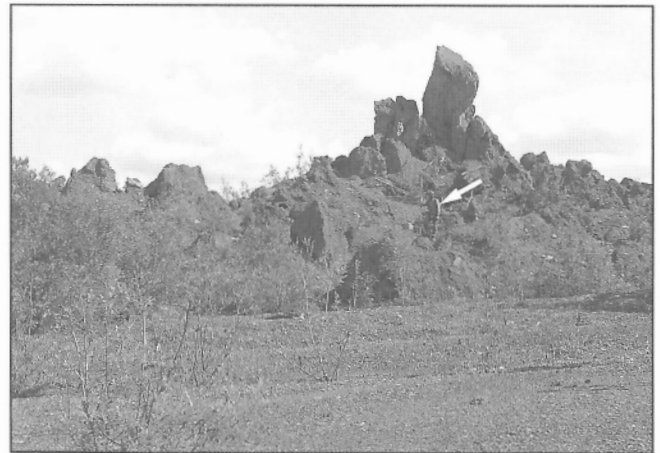


Figure 15. View looking northeast from the relatively flat element 2 to the extreme relief of element 6. The distinctive pinnacle shown here extends >12 m above the surface of element 2. The arrow indicates a man for scale. GSC 1991-118

earthflow that advanced 550 m down a 3° to 7° slope over elements 2 and 4 (Fig. 6 and 17) and also created element 7, a depression behind element 1. This first stage created a chaotic surface of pinnacles and enclosed depressions (Fig. 15 and 18). Relief on this surface of element 6 averages 1.5 to 2 m over 5 m distances but individual pinnacles with reliefs of more than 5 m occur (Fig. 15).

The second stage of formation of geomorphic element 6 was marked by a more fluid earthflow that originated either in element 7 or within the first stage one of element 6. It flowed beyond the margin of stage one onto an old flow surface immediately to the north (Fig. 17).

The third stage of formation of geomorphic element 6 involved the generation of large debris flows in element 7, which cut a head-to-toe channel through the earthflow. The debris flows travelled 300 m down the creek at the toe of the

earthflow (channel gradient 5° to 7°) and spread out onto the lower portion of geomorphic element 4 and into South Macmillan River (Fig. 6 and 17). The flows completely obliterated the forest up to 7m above and 30m on either side of the channel thalweg (Fig. 12). They also formed distinctive nested levee systems (Fig. 12).

Geomorphic element 7

Along with element 3, element 7 is currently the most active area of the landslide. The initial failure that formed elements 6 and 7 resulted in a significant alteration in gradient above element 1. Whereas prior to the failure, the slope above element 1 ran perpendicular to it, within element 7, it now parallels element 1. Consequently, element 7 is expanding rapidly headward (south and west) into the great volume of earthflow and debris flow sediments remaining behind (west



Figure 16. Active failure in the western part of element 3, June 1988. (The arrow indicates a man 1.7 m tall for scale.) GSC 1991-112

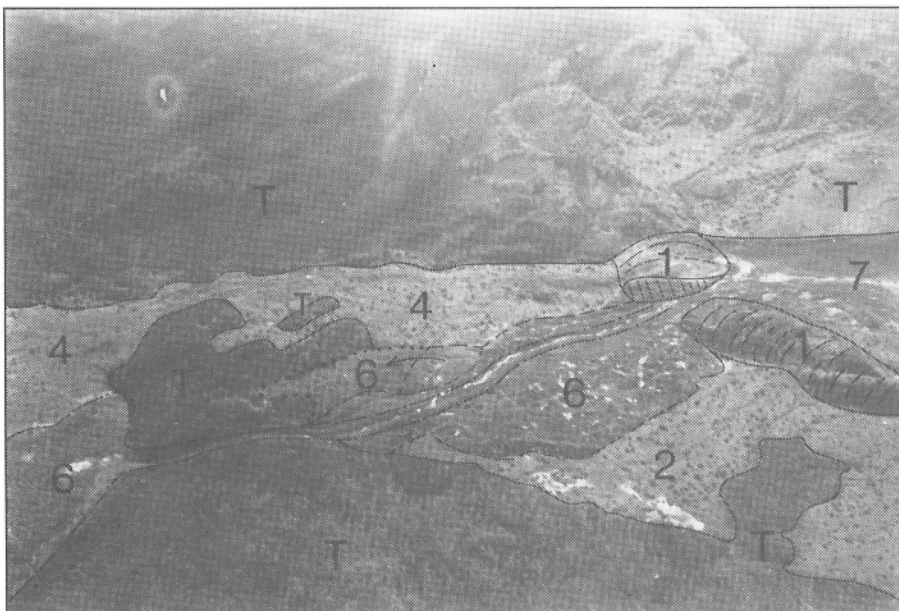


Figure 17. Low-level oblique airphoto of upper part of element 6. Inked lines highlight topography and unit boundaries. The dashed line shows the approximate boundary of the first stage in the formation of element 6. The arrow and dotted line indicate flow direction and the limits of the second stage flow. The dot-dash lines mark the prominent debris flow levee system and debris flow fan created during the third stage. Symbols: T - undisturbed tree covered areas; numbers indicate dendrogeomorphic elements. North is to the left. GSC 1991-076D

of) element 1. Figure 19 shows unsupported material along the back (upslope) margin of element 1 breaking away and moving towards the central depression. A panoramic view from the middle of the depression looking southwest to west (Fig. 20) clearly shows active failure over a slope of $<5^\circ$.

TIMING OF EVENTS

Element 1

Element 1 is the oldest identified feature on the landslide. The distribution of event responses as well as limiting maximum and minimum dates are shown in Figure 21. Maximum dates for the deposition of the landslide colluvium that mantles the ridge are given by radiocarbon dates (Table 2). The average of the three youngest of these dates is 60 radiocarbon years Before Present (1950). Taking the largest error of 80 radiocarbon years and assuming approximate equivalence to calendar years, the landslide colluvium mantle on element 1 formed no earlier than ca. 1810. A minimum date of formation for element 1 is indicated by two scarring events associated with material overflowing the element. Channels A and B (Fig. 3) show events in 1916 ± 3 (tree 86-52) and 1918 ± 3 (tree 86-6), respectively.

Dendrogeomorphic analysis of element 1 is limited, however, by the age distribution of the trees sampled. Few trees from element 1 are old enough to record events in the crucial period from 1810 or later to 1916 (Fig. 22). The only peak in event responses that occurs during this period is 1874 ± 6 and 1875 ± 6 (Fig. 21), with a minor cluster occurring between 1883 ± 5 and 1880 ± 5 . Later peaks in event responses for element 1 were caused by material piling up behind and overflowing that element. A scarring event from the distal part of element 1 in 1874 ± 6 (tree 86-16) and an inclination event in 1875 ± 6 (tree 86-17) indicate that at least this portion of element 1 formed at this time. Trees JK2, JK3, 86-54, and 86-53 also show events in 1874 ± 6 and 1875 ± 6 , which could indicate that this portion of element 1 formed at the same time.

In conclusion, radiocarbon and dendrochronological evidence places the deposition of the landslide colluvium mantle on element 1 at no older than ca. 1810 and no later than ca. 1917 with part of the element formed by ca. 1875.

Elements 2 and 4

The timing of the formation of both elements 2 and 4 is described here. Prior to the formation of element 6, they comprised one continuous element and thus shared similar periods of formation (Fig. 21). Sampling density was relatively high on elements 2 and 4 (Fig. 2), which allows a detailed account of the timing of periods of major flow. Table 3 documents the age of some individual flows that make up elements 2 and 4.

In general, activity on element 2 is clustered during the periods ca. 1914-1922 and ca. 1938-1949 (Fig. 21). The older cluster is only recorded on marginal flows and from parts of element 1 that were disturbed by passing flows (Table 3). This poor documentation is likely the result of the older flow surfaces subsequently being covered by the younger flows. The second period of formation, 1938-1949, is better

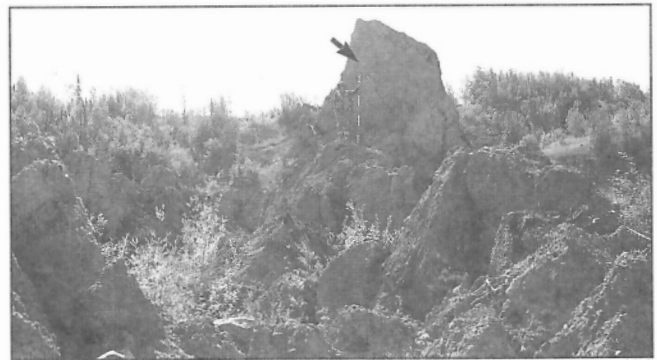


Figure 18. The jumbled, irregular surface of the first stage flow of element 6. GSC 1991-077D



Figure 19. View looking southwest to west from the eastern side of the major failure of element 1 (C of Fig. 6). Landslide material is failing from the back (upslope side) of element 1 into the newly formed depression of element 7. (A 3.7 m ranging pole for scale indicated by the arrow.) GSC 1991-078B, 1991-078C

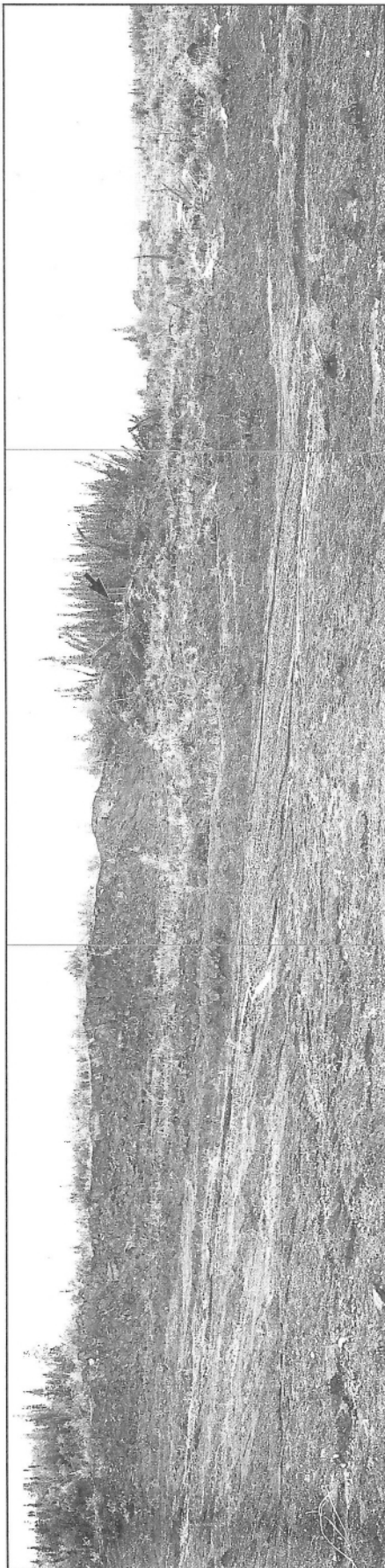


Figure 20. A panoramic view looking southwest from the central portion of element 7. Material is falling along a scarp along towards the centre of element 7. Flow occurs along slopes of 2° to 3°. The treed area in the centre is the same as the treed area in the left centre of Figure 16. (Arrow indicates a person for scale.) GSC 1991-079A, 079B, 079C

represented (Fig. 21) because at this time most of the flows visible in the 1949 airphoto (Fig. 3) were deposited. Comparison between the 1949 and subsequent air photographs (Fig. 4-6) indicate that no major flows were deposited in element 2 after 1949. Thus subsequent peaks in event responses are the result of the unstable nature of the slide material rather than deposition of flows. The main period of formation of element 2 was ca. 1938-1947.

Element 4 formed in similar stages to element 2. Although no early event responses are recorded (Fig. 21), activity is inferred from scarring events on a distal portion of element 1 in 1914 (trees 86-16 and 86-17) and from two inclination events in element 5 (Fig. 21). Again the lack of responses is likely caused by younger flows obliterating trees recording these older events. The growth responses histogram and Table 3 indicate that the main period of formation occurred between 1940 and 1955. The oldest of these flows are those that used to be contiguous with element 2. In general, the next oldest flows are those that flowed down the nested levee system into South Macmillan River forming the debris flow fan. Flows become successively younger in an upslope direction, which indicates that the flows were becoming either less mobile with time or smaller in volume or both; thus they travelled successively shorter distances down the nested levee system. The timing of element 4 flows is detailed in Table 3.

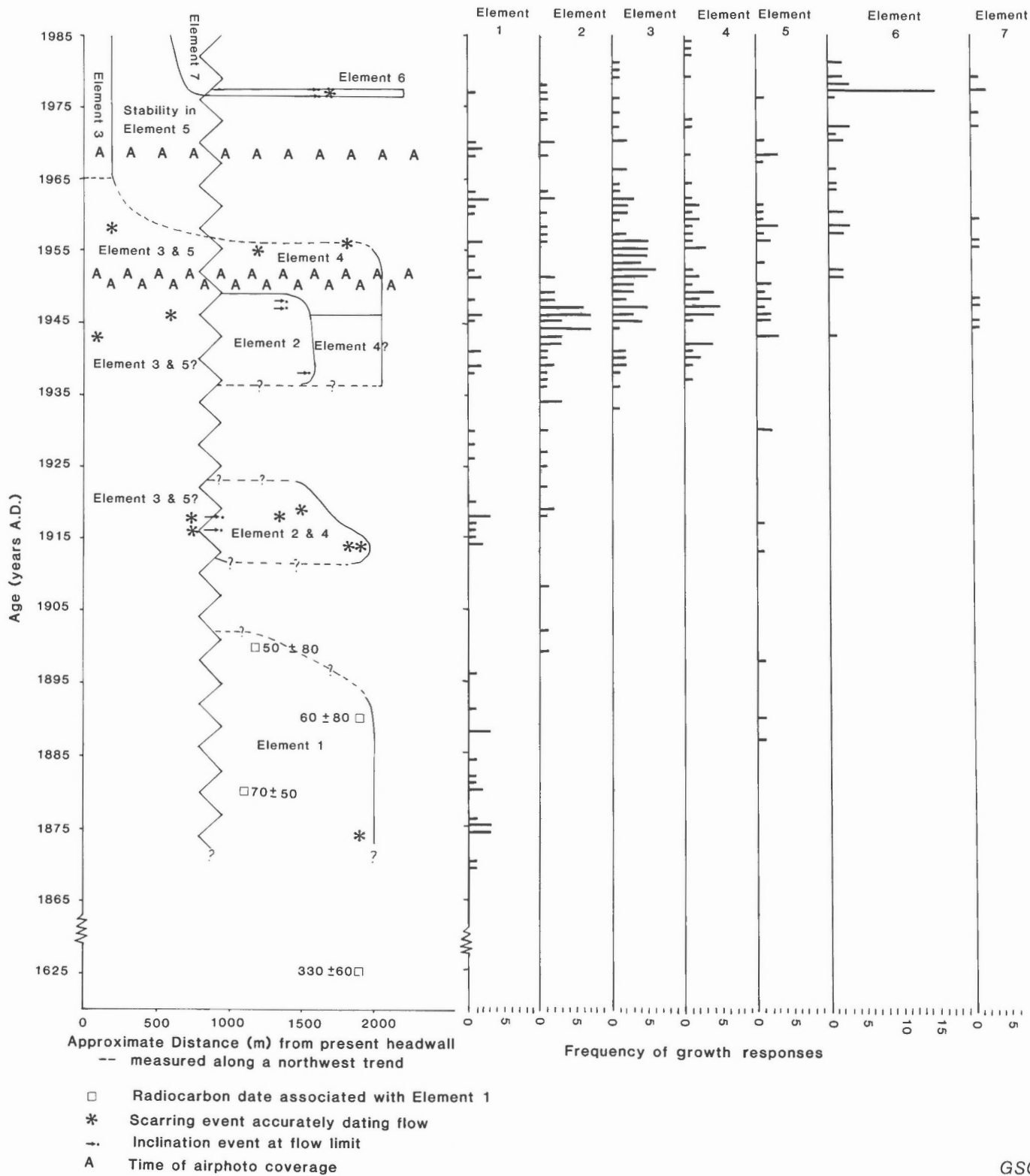
Elements 3 and 5

Elements 3 and 5 served as the source area for material and trees for elements 2 and 4, respectively. Distinctive levees or overflow channels are marked A to I in Figure 3. It is apparent from the age distribution of trees sampled on elements 3 and 5 (Fig. 22) that few old trees survived the repeated slope failures and debris flows that shaped these elements since the formation of element 1 (cf. Fig. 4 and 5). Most were either buried or carried away on pedological soil rafts to lower parts of the slide. This movement explains why no old events are recorded in the growth histogram for element 3 and only a few for element 5. Specific periods of movement are summarized in Table 4. Event responses continued in elements 3 and 5 after elements 2 and 4 became quiescent, which indicates continuing instability in the headwall. Except for active areas marked A and B in Figure 5, the growth response histogram indicates that the rest of elements 3 and 5 had stabilized by 1961 or 1963 although most large failures had probably ceased by ca. 1955

Table 2. Radiocarbon dates from beneath element 1

| Lab number | ¹⁴ C Date ¹ | Material | Comments |
|------------|-----------------------------------|------------------------------------|--|
| GSC-4305 | 70 ± 50 BP | wood (<i>Picea</i>) | Sample obtained from within landslide diamicton |
| GSC-4301 | 330 ± 60 BP | moss (<i>Spagnum</i>) | From same horizon as GSC-4286; excessively old due to hard water effect? |
| GSC-4286 | 60 ± 80 BP | twigs (<i>Salix</i>) | Agrees with GSC-4305 and -4289 |
| GSC-4289 | 50 ± 80 BP | wood fragments (<i>Picea</i>) | Sample from outermost rings of a log within landslide diamicton |

¹ All dates are corrected for $\delta^{13}\text{C}$ fractionation with the exception of GSC-4286.



GSC

Figure 21. Composite event/response diagram.

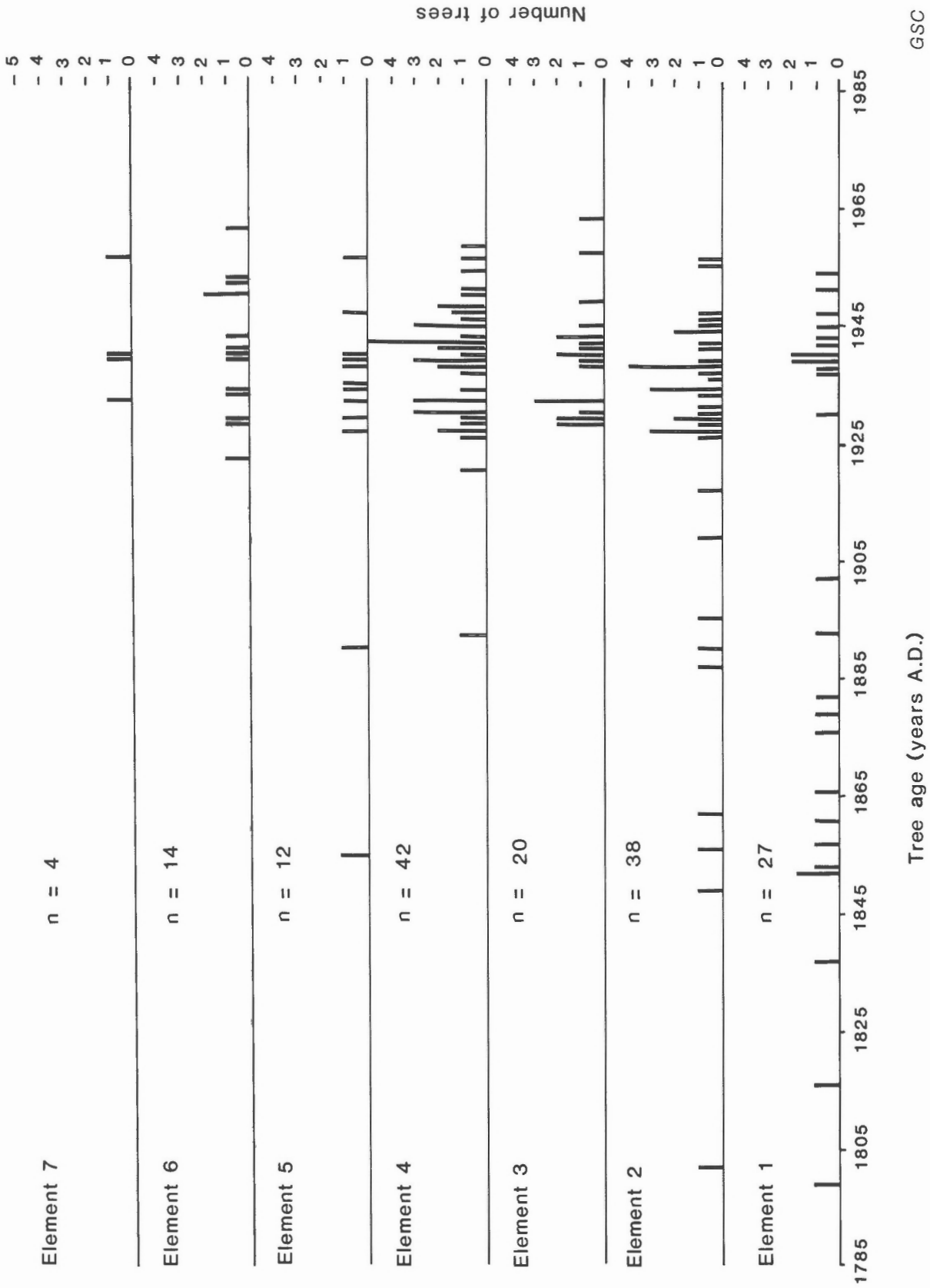


Figure 22. Frequency plot for the ages of trees used to date events during the evolution of the Surprise Rapids landslide.

Table 3. Flow chronology for elements 2 and 4

| Element | Flow number (Fig. 3-5) | Period of activity (years A.D.) | Documentation (Trees located in Fig. 2) | Comments |
|---------|---------------------------|------------------------------------|--|--|
| 2 | I | ca. 1914-1922 | Scarring events in trees 86-6, 86-16, 86-17, 86-46, 86-48, 86-50, 86-52 | Trees 86-6 and 86-52 associated with overflow channels A and B (Fig. 4, 5) |
| 2 | II | ca. 1938-1940 | Inclination events in trees 86-46, 86-49, 86-50 | Synchronous activity on element 4; growth responses noted on scattered trees growing on element 4 but no flow surface defined with certainty |
| 2 | III | ca. 1944 | Inclination event in tree 86-42 | Flow III overlies flow II and is overlain by flow IV |
| 2 | IV | ca. 1946-1947 | Inclination event in trees 86-37, 86-38 | Airphotos indicate no major flows on element 2 between 1949 and 1968; growth response histograms (Fig. 21) indicate continuing instability within flows until ca. 1956 |
| 4 | V | ca. 1940-1945 | Event response in tree BG-5 | Trees dated as older than 1945, 1947, 1948 show no disturbance; older flows may have occurred on element 4 but were buried by younger flows |
| 4 | VI | ca. 1940? | Underlies flow VII and is fresh and unvegetated in 1949 airphoto | Flow entered South Macmillan River and changed its course resulting in formation of bar "a" (Fig. 4) |
| 4 | VII | ca. 1946 | Inclination event in trees DF-4, Z-2, Z-5 | |
| 4 | VIII | ca. 1949 | Overlies flow VII and predated 1949 airphoto coverage; scarring event tree DF-6 and inclination event tree AB-12. | |
| 4 | X | ca. 1949 | Dark tone (high water content) indicates flow to be contemporary with 1949 airphoto | |
| 4 | XI | ca. 1950 | Inclination events trees AB-1, AB-2; flow not present in 1949 airphoto but present in 1950; dark tone indicates high water content | |
| 4 | XII | ca. 1952 | Postdates 1950 airphoto; scarring event tree DF-1 | Blocked levee that conducted flow XI caused avulsion of subsequent flows XIII and XIV in this area of element 4 |
| | XIII | ca. 1954 | Three inclination events B6-2, B0-4, AB-6 | |
| | XIV | ca. 1955 | Scarring event tree 86-19 plus three inclination events 86-10, 81-21, CT-3 | Surface of element 4 stable by 1955 |



Figure 23. Headward sapping by springs along element 1. (A) View down from rim of element 1 of the area of transition from brittle slumped sediment to debris flow; dashed lines mark debris flow levees. (B) Looking toward the face of element 1; fresh slumping, directly behind the senior author has occurred as a result of undermining by spring activity visible beneath his feet. GSC 1991-111



Table 4. Failure event chronology for elements 3 and 5

| Element | Flow of failure area (Fig. 4 to 6) | Period of activity (years A.D.) | Documentation (Trees located in Fig. 1) | Comments |
|---------|---------------------------------------|------------------------------------|--|--|
| 3 | Entire element | ca. 1939-1942 | Many inclination events; refer to Fig. 21 | Associated with early second phase of element 2 |
| 3 | Entire element | ca. 1945-1987 | Many inclination events; refer to Fig. 21 | Associated with peak of flow emplacement for element 2 |
| 3 | IX | ca. 1946 | Inclination events trees 86- 8, 86-9 | Flow emplacement caused instability in element 1 (inclination event tree 86-7) |
| 3 | Portion of headscarp | Now active | Compare Fig. 4 and 5 | Flows from headwall continued to load southwest margin of element 1 |
| 5 | Entire element | ca. 1913-1917 | Two inclination events; trees X-7, X-9 | Likely associated with formation of element 4 |
| 5 | J | ca. 1943-1961 | Many inclination events; refer to Fig. 21; contemporaneous movement recorded on 1949 and 1950 airphotos (cf. Fig. 3 to 4) | Corresponds to last phase of flow activity on element 4 ca. 1945-1955; forest area (J on Fig. 4) was chief source of debris and trees for element 4 |
| 5 | XV | ca. 1955-1957 | Two inclination events; trees B0-5, X-10 | Final flow to leave element 5 |
| 5 | XVI | ca. 1956 | Two inclination events; trees X-2, X-3 | Last earthflow to occur within element 5 before cessation of instability |

(Table 4). The last major failures removed the remaining undisturbed forested areas (J and K of Fig. 4) between 1950 (the year Fig. 4 was taken) and ca. 1955.

Elements 6 and 7

As mentioned previously, element 6 formed in three phases during 1977, and, assuming a mean thickness of 2 m consists of an estimated $3.6 \times 10^4 \text{m}^3$. The creation of the pinnacled terrain during phase 1 was recorded by injuries to trees CT-6 and X-12. Phase 2 was dated by tree X-11. The maximum stage of levee formation scarred and inclined trees 86-1 and 86-2 in 1977 (Fig. 12).

Geomorphic element 7 was created simultaneously with element 6 and is currently failing actively (Fig. 19 and 20). Failure here will likely continue until debris flow and earthflow sediments accumulated behind element 1 have flowed out through the breach created during the formation of element 6.

CHRONOLOGY AND MODES OF FAILURE OF SURPRISE RAPIDS LANDSLIDE

Geomorphic development of Surprise Rapids landslide are divided into two phases for the convenience of discussion: initial slope instability, which led to failures in elements 3 and 5 and the ponding of landslide colluvium behind element 1, and subsequent failures (including those documented on air photographs).

Initial failures

The causes of the initial failures in elements 3 and 5 are unclear. Two possibly coactive factors are proposed: First, an extensive forest fire swept the area sometime before the landslide began. Burnt logs and charcoal are common within the landslide colluvium. Charred and fallen or dead-standing trees litter the floor of the present forest in areas surrounding the landslide. Possibly the fire was intense enough to burn off the insulating layer of lichens and mosses, which blanketed the preexisting slopes in the area of elements 3 and 5. This exposure could have initiated thaw-related failures. The second factor may have been climatic warming. The inundation of element 1 approximately coincides with the start of a trend of climatic amelioration in Alaska and Yukon which began in the 1850s and continued until ca. 1950 (Thomas, 1961; Garfinkel and Brubaker, 1980; Jacoby and Cook, 1981; Allen, 1982; Cropper, 1982). Some indication of the magnitude of the change is provided by Garfinkel and Brubaker (1980) and Cropper (1982). Their analyses of dendrochronological proxy data indicate that summers in the interior of Alaska during the first half of the Twentieth Century were between 2.1° and 3°C warmer than during the last half of the Nineteenth Century. Advance of the treeline reported by Griggs (1937) correlates with this warming trend;

permafrost degradation in Mackenzie Mountains immediately east of the South Macmillan basin is at least partly contemporaneous (Kershaw and Gill, 1979).

Initial failure and climatic amelioration may be entirely coincidental; we cannot show that climatic warming triggered the initial failure. However, the failure does correlate with the period when thaw-related instability was sustained and, occasionally, accelerated.

Contemporary failure

Contemporary failure modes include failure of undisturbed slope materials in the headscarp of element 3, localized slumping and catastrophic failure of element 1 and the landslide colluvium ponded behind it, and continued remobilization of landslide colluvium in element 7.

Headscarp failure

The southwestern portion of the element 3 headscarp is the only location within the landslide complex where the melting of ground ice in undisturbed material can be linked directly to failure. As previously noted, interstratified ice and segregated ice lenses have been observed in the silt and clay-rich glacial diamicton exposed in the headscarp. Melting of this ice-rich soil produces excess water, which contributes to immediate sloughing of thawed soil off the steep headscarp. The colluvium that accumulates at the bottom of the headscarp is fine grained and has a high bulk moisture content and low in situ strength. It is also characterized by poor internal drainage and the presence of free water. Because of these conditions, the colluvium is unstable and moves slowly downslope as an earthflow. The mode of failure therefore includes both ablation of the headscarp and flow of thawed material on a gentle slope away from the headscarp. This type of mass movement has been described as a bimodal flow by McRoberts and Morgenstern (1973, 1974a, b).

The unstable colluvium currently descends element 3 as a slow-moving, partly vegetated earthflow. This flow is in marked contrast to more mobile flows in the 1940s (Fig. 3, 4, and 21), which descended element 3, flowed across element 1, and continued a kilometre beyond down slopes of only a few degrees to form element 4. McRoberts and Morgenstern (1974a, b) have shown the mobility of thawing sediments to be directly related to their ice contents. The decreased mobility of bimodal flows in element 3 likely indicates a lower content of segregated and interstitial ice within the glacial diamicton now exposed in the headscarp compared with sediments exposed during the 1940s.

Elsewhere along the headscarps of elements 3 and 5, we found no recent evidence of thaw-related failure or groundwater discharge, although we noted locally some dry pipes, probably related to the seasonal conductance of snow meltwaters and rainwater. Retreat has apparently ceased altogether, which we believe to be the result of further diminished content of ground ice in these areas. We consider

that the distribution of ground ice in the slope above the headscarp of the landslide is now the prime control on its ultimate size.

Failure of element 1

The causes of the catastrophic failure of element 1 and the creation of elements 6 and 7 are not clear. The morphology of element 6 indicates that two modes of failure occurred concurrently during its formation. The upper 3 to 5 m or more of the mass was brittle and failed by fracture and foundering, whereas the base had extremely low strength and probably flowed like a viscous fluid, as evidenced by the low gradient of slope over which the failure occurred. The brittle upper part of the flow progressively foundered into the low strength base as the flow advanced and thinned (Fig. 15, 17, 18, 19). A third mode followed, characterized by mobile earthflow and debris flow that lacked a brittle crust (Fig. 6 and 12).

The superposition of brittle colluvium over a slurry-like substrate likely reflects a pre-failure stratigraphy in the deposits behind element 1. Such a stratigraphy is not unexpected. Large quantities of earthflow and debris flow sediments accumulated upslope of element 1 during the rapid headward growth of elements 3 and 5 prior to ca. 1955. The rapid accumulation of these deposits likely exceeded the rate at which permafrost formed within them. As accumulation waned, permafrost penetrated the sediments creating a frozen, brittle, moderately consolidated crust over an unfrozen poorly consolidated substrate. Furthermore, element 1 may have originally impounded a small body of water or fen or bog along at least part of its length before any slope instability began in the area. If so, subsequent slope failures ponded behind element 1 would have rested upon an underconsolidated substratum of very low strength. The presence of an extensive pond with an accumulation of fine sediment at its base within the landslide area prior to failure would explain the anomalously high clay contents within the landslide diamicton.

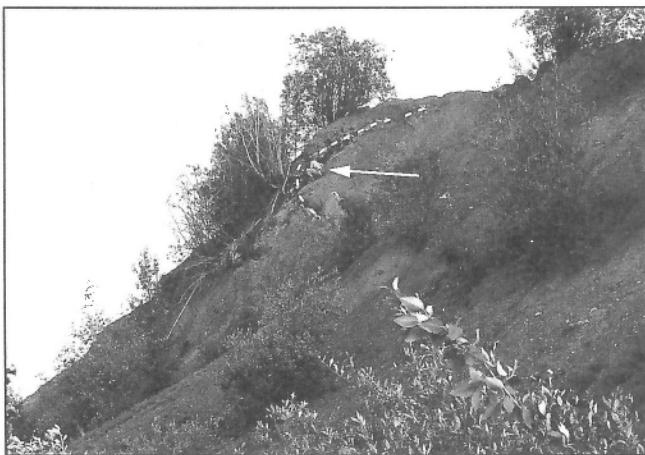


Figure 24. The dashed line traces and overturned bed of the White River Tephra in the face of element 1. (The arrow indicates a man for scale.) GSC 1991-119

The failure of element 1 could have been caused by one or some combination of the following conditions:

- a) Fluvial erosion of a channel through element 1. Fluvial erosion was concentrated between debris flow levees (I of Fig. 3) and breached element 1. Possibly a larger breach was cut by fluvial erosion at the head of element 6 (H of Fig. 3). This erosion could have weakened element 1 until it failed or allowed the initiation of outflow of the low strength base of element 6, which rapidly enlarged the breach to the point of catastrophic failure.
- b) Progressive weakening of element 1 as a result of localized instability affecting the steep toe. This process is currently underway (B to C of Fig. 3 and 23) and may be analogous to the processes leading to the failure of element 1 and the formation of element 6. In this area, groundwater discharges at midslope and causes shallow sloughing. The groundwater may originate from ponds in numerous closed depressions upslope and pass either through deep flow or paths through an active layer; the groundwater may alternatively indicate thermal degradation of ground ice. The colluvium is progressively remolded into debris flows that flow down the face of element 1. The face of element 1 is thus undermined causing the slope face to retreat along an amphitheatre-like margin about 15 m across. This process systematically reduces the lateral strength of element 1 and, in the extreme, will breach it. Both circumstances could result in the catastrophic failure of fluid landslide colluvium behind element 1.
- c) High lateral loads imposed by the rapid buildup of fluid colluvium behind element 1. These loads could have caused creep and eventually creep rupture (McRoberts and Morgenstern, 1974b; Savigny and Morgenstern, 1986b, c) in permafrost soils comprising element 1. Alternately, shear stresses caused by the high lateral load coupled with high pore pressures and decreased effective stresses associated with aggradation of permafrost may have simply exceeded the



Figure 25. Standing water of element 7. GSC 1991-116

shear strength of soils comprising element 1. Field evidence documents deformation of the glaciofluvial gravel core and at least part of the landslide colluvium mantle of element 1 possibly from lateral loading. In Figure 24 (G of Fig. 3) the pre-landslide forest floor marked by the White River Tephra and overlying landslide colluvium are overturned along the face of element 1.

Regardless of what caused the breach of element 1, the result appears analogous to the breach of an earth dam. Fluid material oozed through the chute carrying a brittle crust passively above it. After passing through the chute, the brittle crust broke into discrete blocks or rafts. Some rafts simply

became grounded, others were stacked while others became temporary dams that were ultimately toppled and deformed as fluid material built up behind them. The subsequent earthflow and debris flows that crossed element 6 during the same year (1977) may have been caused either by failure of isolated pockets of unfrozen colluvium remaining behind element 1, or by continued bimodal flow activity.

Remobilization

Remobilization of landslide colluvium is occurring in element 7. Failure at the headwall of element 7 (Fig. 20) begins with tension cracking, which progresses into slumping

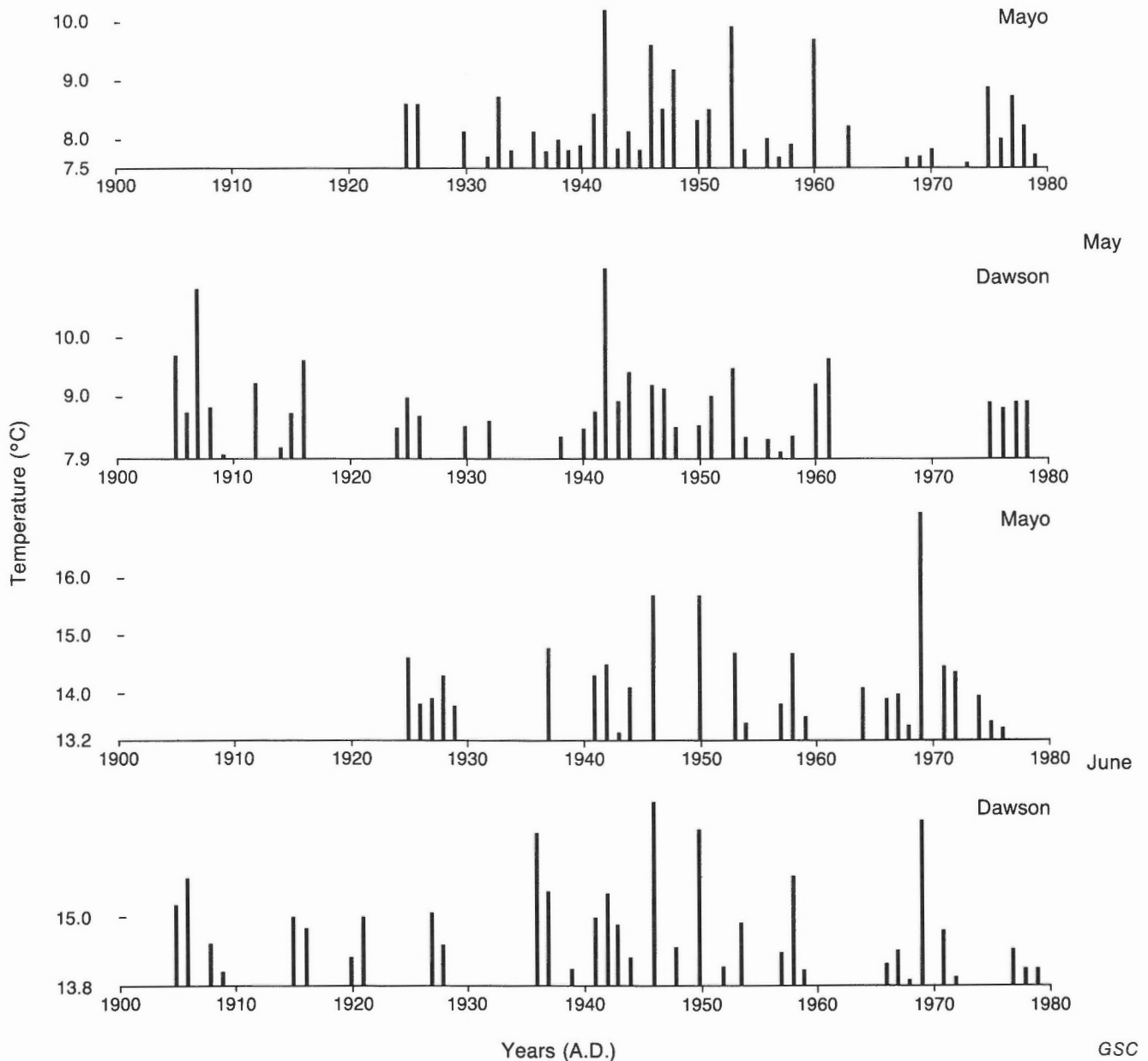


Figure 26. Mean monthly temperatures for Dawson and Mayo weather stations in excess of averages for the period 1900-1979 (Dawson) and 1925-1979 (Mayo). The dashed line marks one standard deviation above the mean. Elevations and locations for the stations: Dawson (504 m, 64°3'N, 139°26'W) and Mayo (504 m, 63°37'N, 135°52'W) (Data courtesy of Environment Canada).

and toppling. This deformation style is particularly active during the late spring and early summer when seasonal thaw, snow melt, and rainy weather have saturated landslide sediments and extensive areas of standing water exist on element 7 (Fig. 25). Slumped and toppled sediments grade progressively downslope into earthflows that creep toward the breach in element 1. The gradient of the slope in this area is $<5^\circ$. Much of the colluvium in element 7 was deposited during the 1940s. The soils are expected to comprise a thick wedge of material with a high bulk moisture content. The extent of permafrost in this wedge and the type of ground ice present in this permafrost is unknown and could be confirmed only through drilling.

DISCUSSION

Bimodal flows, or retrogressive slides as they are sometimes called, are commonly associated with fine grained glaciolacustrine sediments and thermokarst terrain in valley bottom settings (e.g., McRoberts and Morgenstern, 1974a; Klassen, 1979; Burn et al., 1986). Studies of slope stability problems associated with permafrost commonly focus on such glaciolacustrine soils (e.g., Savigny and Morgenstern, 1986a, b, c).

Surprise Rapids landslide is of particular interest because it occurred at a midslope location over relatively gentle slopes and in a forested plateau setting where drift rests directly on bedrock. The rapid growth and exceptional size of this landslide illustrate the potential for large mass movements, associated with development-related disturbance, to occur on similar slopes elsewhere in the region. The landslide may also provide a glimpse of the potential widespread effect of global warming on the stability of ice-rich permafrost soil and rock in montane areas.

Although the ultimate triggering mechanism for instability is unknown, its occurrence at this site rather than similar nearby hillsides may have been determined by the higher ice content of the clayey glacial sediments underlying the slope prior to failure. Once thaw was initiated, the low shear strength and loamy texture of the sediments ensured rapid growth of the landslide even on gentle slopes. Furthermore, whereas climatic amelioration cannot be shown conclusively to be responsible for initially triggering the landslide, it likely played a role in the rapidity of permafrost degradation once initial slope failures had occurred. The most active period of landslide growth was from the late 1930s to the early 1950s. During this time, four and five of the warmest months of May and June were recorded at Dawson and Mayo (Fig. 26). Warm weather during these months would serve to accelerate not only the melting of the winter snow pack but also the thaw of seasonally frozen landslide colluvium and permanently frozen sediment in retreating headscarps.

CONCLUSIONS

The Surprise Rapids landslide is a complex of earthflows and debris flows. Failure is confined to the surficial covering of glacial deposits with no known involvement of bedrock. The

mechanism of initial failure is uncertain but subsequent growth involved bimodal flows and reactivation of resulting colluvium in the form of earthflows, debris flows, and, possibly translational sliding. Bimodal flows remain active locally along the landslide headscarp. Much of the headscarp has stabilized and it is proposed that the development of bimodal flows in these areas ceased at the limit of extensive interstitial and segregated ground ice. The landslide colluvium has a clay content about twice that of glacial diamictons that mantle the Yukon Plateau in the surrounding region.

Mass movements at this site began by the 1870s. Earthflow and debris flow activity built aprons and fans during the second, fourth, and the seventh decades of this century.

The cause of initial failure is not known. Landsliding followed a major forest fire that swept the area and has been contemporaneous with a period of climatic amelioration. These two may have been factors in landslide initiation and acceleration.

The rapid growth and exceptional size of the Surprise Rapids landslide are seen as an example of the potential instability of hillsides with similar slopes and aspects on the Yukon Plateau.

ACKNOWLEDGMENTS

The authors gratefully acknowledge the help of Dr. Bea Alt in directing us to the climatic literature for Alaska and Yukon; Environment Canada provided the tabulated climatic data. Thanks is also extended to John Witham, for without his extraordinary fixed wing and helicopter flying skills, this study would not have been possible.

REFERENCES

- Alestalo, J.**
1971: Dendrochronological interpretation of geomorphic processes; *Fennia*, v. 105, p. 1-140.
- Allen, H.D.**
1982: Dendrochronological studies in the Slims River Valley, Yukon Territory; unpublished MSc thesis, University of Calgary, Calgary.
- Burn, C.R., Michel, F.A., and Smith, M.W.**
1986: Stratigraphic, isotopic, and mineralogical evidence for an early Holocene thaw unconformity at Mayo, Yukon Territory; *Canadian Journal of Earth Sciences*, v. 23, p. 794-803.
- Burrows, C.J. and Burrows, V.L.**
1976: Procedures for the study of snow avalanche chronology using the growth layers of woody plants; University of Colorado, Institute for Arctic and Alpine Research, Occasional Paper 23, p. 1-54.
- Carrara, P.E.**
1979: The determination of snow avalanche frequency through tree-ring analysis and historical records at Ophir, Colorado; *Geological Society of America, Bulletin*, v. 90, p. 773-780.
- Cropper, J.P.**
1982: Climate reconstructions (1801-1938) from tree-ring chronologies of the North American Arctic; *Arctic and Alpine Research*, v. 14, p. 223-241.
- Gabrielse, H.**
1967: Tectonic evolution of the northern Canadian Cordillera; *Canadian Journal of Earth Sciences*, v. 4, p. 271-297.
- Garfinkel, H.L. and Brubaker, L.B.**
1980: Modern climate-tree-growth relationships and climate reconstruction in sub Arctic Alaska; *Nature*, v. 286, p. 872-874.

- Griggs, R.F.**
1937: Timberlines as indicators of climatic trends; *Science*, v. 85, p. 251-255.
- Jackson, L.E., Jr.**
1977: Dating and recurrence frequency of prehistoric mudflows near Big Sur, Monterey County, California; U.S. Geological Survey, *Journal of Research*, v. 5, no. 1, p. 17-32.
- Jacoby, G.C. and Cook, E.R.**
1981: Past temperature variations inferred from a 400-year tree ring chronology from Yukon Territory, Canada; *Arctic and Alpine Research*, v. 13, p. 409-418.
- Johnston, G.H., ed.**
1981: Permafrost engineering design and construction; John Wiley and Sons, Canada Limited, Toronto, 540 p.
- Kershaw, G.P. and Gill, D.**
1979: Growth and decay of palsas and peat plateau in the Macmillan Pass-Tsichu River area, Northwest Territories, Canada; *Canadian Journal of Earth Sciences*, v. 16, p. 1362-1374.
- Klassen, R.W.**
1979: Thermokarst terrain near Whitehorse, Yukon Territory; in *Current Research, Part A*, Geological Survey of Canada, Paper 79-1A, p. 385-388.
- La Marche, V.C., Jr.**
1961: Rate of slope erosion in the White Mountains, California; *Geological Society of America, Bulletin*, v. 72, p. 1579.
1966: An 800-year history of stream erosion as indicated by botanical evidence; U.S. Geological Survey, Professional Paper 550-D, p. 83-86.
- La Marche, V.C., Jr. and Wallace, R.E.**
1972: Evaluation of effects on trees of past movements on the San Andreas Fault, northern California; *Geological Society of America, Bulletin*, v. 83, p. 2665-2676.
- Lawrence, D.B.**
1950: Estimating dates of recent glacier advances and recession rates by studying tree growth layers; *Transactions, American Geophysical Union*, v. 31, p. 243-248.
- McRoberts, E.C. and Morgenstern, N.R.**
1973: A study of landslides in the vicinity of the Mackenzie River mile 205-660; Environmental-Social Committee Northern Pipelines, Task Force on Northern Development, Report no. 73-35, 96 p.
1974a: The stability of thawing slopes; *Canadian Geotechnical Journal*, v. 11, p. 447-469.
1974b: Stability of slopes in frozen soil, Mackenzie Valley, N.W.T.; *Canadian Geotechnical Journal*, v. 11, p. 554-573.
- Miller, D.J.**
1960: Giant waves in Lituya Bay, Alaska; U.S. Geological Survey, Professional Paper 354-C, p. 51-86.
- Morgenstern, N.R. and Smith, L.B.**
1973: Thaw-consolidation tests on remolded clays; *Canadian Geotechnical Journal*, v. 10, p. 25-40.
- Permafrost Subcommittee**
1988: Glossary of permafrost and related ground ice terms; National Research Council, Associate Committee on Geotechnical Research, Technical Memorandum no. 142, 156 p.
- Pierson, T.C. and Costa, J.E.**
1987: A rheologic classification of subaerial sediment-water flows; in *Debris Flows/Avalanches: Process, Recognition, and Mitigation*, J.E. Costa and G.F. Wieczorek (ed.); *Reviews in Engineering Geology*, v. VII, Geological Society of America, Boulder, p. 1-12.
- Potter, N.**
1969: Tree-ring dating of snow avalanche tracks and the geomorphic activity of avalanches, northern Absaroka Mountains, Wyoming; INQUA Volume, Geological Society of America, Special Paper 123, p. 141-165.
- Savigny, K.W. and Morgenstern, N.R.**
1986a: Geotechnical condition of slopes at a proposed pipeline crossing, Great Bear River valley, Northwest Territories; *Canadian Geotechnical Journal*, v. 23, p. 490-503.
1986b: In situ creep properties in ice-rich permafrost soil; *Canadian Geotechnical Journal*, v. 23, p. 504-514.
1986c: Creep behaviour of undisturbed clay permafrost; *Canadian Geotechnical Journal*, v. 23, p. 515-527.
- Shroder, J.F. Jr.**
1975: Dendrogeomorphological analysis of mass movement; *Proceedings of the Association of American Geographers*, v. 7, p. 222-226.
1978: Dendrogeomorphological analysis of mass movements on Table Cliffs Plateau, Utah; *Quaternary Research*, v. 9, p. 168-185.
1980: Dendrogeomorphology: review and new techniques of tree-ring dating; *Progress in Physical Geography*, v. 4, p. 1961-1988.
- Sigafoos, R.S.**
1964: Botanical evidence of floods and floodplain deposition; U.S. Geological Survey, Professional Paper 485-A, p. 1-35.
- Stokes, M.A. and Smiley, T.L.**
1968: An introduction to tree-ring dating; University of Chicago Press, Chicago, Illinois, 73 p.
- Thomas, M.K.**
1961: A survey of temperatures in the Canadian Arctic; in *Geology of the Arctic*, G.O. Raasch (ed.); University of Toronto Press, Toronto, p. 942-955.
- Viereck, L.A.**
1965: Relationship of white spruce to lenses of perennially frozen ground, Mount McKinley National Park, Alaska; *Arctic*, v. 18, p. 262-267.

APPENDIX 1

Responses of trees to geomorphic processes

In using tree ring analysis, it is important to understand the growth and anatomy of trees. The reader is directed to Burrows and Burrows (1976) for a primer on the fundamentals of this subject.

To date a geomorphic process, the process must produce an event or a number of events that affect a tree's growth sufficiently to produce a growth response. Geomorphic processes produce seven basic events as follows: (1) inclination; (2) shear of rootwood or stemwood; (3) corrosion; (4) burial of stemwood; (5) exposure of rootwood; (6) inundation; and (7) nudation (Shroder, 1980). Any of these events can produce one or more of the following growth responses: (a) reaction-wood growth; (b) scarring; (c) growth suppression or growth release; (d) sprouting; (e) miscellaneous structural and morphological changes in external or internal wood character; and (f) succession (Shroder, 1980). All these growth responses can be used to date geomorphic processes. Dendrogeomorphological study of the Surprise Rapids landslide was limited to reaction-wood growth and scarring.

Scarring

Scarring is caused by disruption or removal of the vascular cambium (Shroder, 1978). Shear or rupture of the root-wood disrupts the cambium whereas extensive corrosion of the bark

removes part of the cambium (Shroder, 1978). This damage produces distinctive scars that can be dated (Fig. 7). After the wood has been exposed, callous tissue forms around the margin of scar and eventually covers it (Sigafos, 1964).

Reaction wood growth

Reaction wood forms in response to the inclination of a tree as it attempts to return its upper growth to vertical (Shroder, 1980). This growth is a geotropic (gravity-growth controlled) response, which is caused by growth hormones becoming concentrated on the lower side of the inclined trunk and stimulating increased growth (Sigafos, 1964). Reaction wood yields the most accurate dates because delayed responses are generally uncommon (Potter, 1969; Shroder, 1975, 1978, 1980; Burrows and Burrows, 1976; Carrara, 1979).

The character and description of reaction wood are discussed by Burrows and Burrows (1976). In gymnosperms, reaction wood is referred to as compression wood. Reaction wood occurs as eccentric tree rings on the lower side of the inclined trunk in the direction of tilting. Besides the rings being much thicker on one side of the pith than on the other side, they are denser and darker (Fig. 9A and B). The presence of complex reaction wood (Fig. 8) indicates several episodes of inclination or rotation, or both.

